

ANTENNA-PLASMA COUPLING THEORY FOR ICRF HEATING  
OF LARGE TOKAMAKS\*

A. Bers, L. P. Harten and A. Ram

PFC/RR-81-7

February 1981

# ANTENNA - PLASMA COUPLING THEORY FOR ICRF HEATING OF LARGE TOKAMAKS\*

A. Bers, L. P. Harten, and A. Ram, M.I.T. Plasma Fusion Center, Cambridge, MA 02139

The radiation impedance of, and field excitation by, current sheets external to a large (minor radius) plasma are calculated. The finite-size antenna current modeled by these current sheets is screened from the plasma by a sheath of anisotropic conductivity which shorts out locally the toroidal rf electric field but does not affect the poloidal rf electric field. The plasma near the antenna is modeled by its cold dielectric tensor having an inhomogeneous density and applied magnetic field. The field analysis for the coupling and power flow is carried out in a slab geometry.

In ICRF heating of tokamaks the coupling of external rf power to the plasma is achieved by introducing rf current carrying conductors near the plasma wall in the shadow of the limiter. Effective coupling is usually achieved when these rf current carrying conductors are shielded from the plasma by a metal screen which shorts out the toroidal rf electric fields. The screen also prevents the plasma from penetrating to the rf current carrying conductor. In an attempt at an analysis of such a coupling structure, the simplest model is to consider a current sheet antenna which is placed between a highly conducting wall and a sheet of anisotropic conductivity representing the screen, as shown in Fig. 1. The low density inhomogeneous (in  $x$ ) plasma in the shadow of the limiter is then assumed to exist to the right of this screen. The excitation of the fields in the plasma can be studied by analyzing the radiation properties of this current sheet antenna structure. For this we assume that the sheet current distribution on the antenna is given and that the fields excited in the plasma are absorbed on a single pass. For large (minor radius) tokamaks the simplest analysis can be carried out in slab geometry and the relevant plasma equations near the antenna can be solved in the WKB approximation with proper attention given to any possible turning points that represent cutoffs in that vicinity. An outline of such a field analysis was recently given.<sup>1</sup> We have now carried out the details of the analysis and present here the results as well as computations based upon these analytical results.

The elementary current sheet is assumed to carry a current in the  $y$  (poloidal) direction and to have a given variation in the  $y$  (poloidal) and  $z$  (toroidal) directions at a frequency  $\omega$ :

$$\vec{K} = \hat{y}K_0 f(y)g(z) \leftrightarrow \hat{y}K_0 F(k_y)G(k_z) \quad (1)$$

where  $K_0$  is the complex amplitude of the current (Amp/m), and  $F$  and  $G$  are the Fourier transforms of  $f$  and  $g$ . The fields in the free space region, containing the current sheet, between the wall and the screen are described by a superposition of the full set of TE and TM modes.<sup>1</sup> The TEM fields related to the feed of the current sheet are ignored. Just to the right of the screen the fields in the inhomogeneous plasma are described by<sup>1</sup>

$$\frac{d^2 E_y}{d\xi^2} + n_\xi^2(\xi)E_y = 0 \quad (2)$$

$$n_\xi^2 = (K_\perp - n_{yz}^2) + K_\times^2/(n_z^2 - K_\perp) \quad (3)$$

$\xi = k_0 x$  with  $k_0 = \omega/c$ ,  $n_{yz}^2 = n_y^2 + n_z^2$ , with  $n_y = k_y/k_0$ ,  $n_z = k_z/k_0$ , and  $K_\perp(\xi)$  and  $K_\times(\xi)$  are the usual

\* Work supported by U.S DOE contract DE-AC02-78ET-51013.

normalized dielectric functions of the cold plasma dielectric tensor. Equation (2), appropriate for studying the fast-wave excitation, ignores the  $E_z$ -field in the plasma and terms containing derivatives of the dielectric functions. In the vicinity of the screen ( $\xi = \xi_{\text{scr}}$ ) we let  $n_\xi^2 = \alpha_1 + \alpha_2 \xi$ ,  $\alpha_1 = n_\xi^2(\xi_{\text{scr}}) - \xi_{\text{scr}} \alpha_2$  and  $\alpha_2 = (dn_\xi^2/d\xi)$  at  $\xi = \xi_{\text{scr}}$ . The solution to (2) having outgoing waves into the plasma is then

$$\Gamma_y = E_0[\text{Ai}(\tau) - i \text{Bi}(\tau)] \quad (4)$$

where Ai and Bi are the usual Airy functions, and

$$\tau = -(\alpha_1 + \alpha_2 \xi)/\alpha_2^{2/3}. \quad (5)$$

The cutoff ( $n_\xi^2 = 0$ ) in the plasma near the screen occurs at  $\xi = -\alpha_1/\alpha_2$ . In the following we shall assume that the plasma density at the screen, although very small, is nonzero so that we can ignore the slow wave resonance at  $n_z^2 = K_\perp \approx 1$ . Equation (4) together with the free-space fields around the current sheet can be used to satisfy the boundary conditions at the wall, screen, and current sheet. There are nine such boundary conditions, giving the complex field amplitudes  $E_{\pm a}$ ,  $H_{\pm a}$ ,  $E_{\pm b}$ ,  $H_{\pm b}$ , and  $E_0$  in terms of the current sheet complex amplitude  $K$ . From these we can determine the radiation impedance of the current sheet antenna and the fields and power flow into the plasma.

The radiation impedance of the antenna,  $Z_A = R_A + iX_A$ , is obtained by applying the complex Poynting theorem at the surface of the radiating current sheet:

$$\begin{aligned} Z_A &= \frac{2}{|I|^2} \int dy \int dz \left( \frac{1}{2} E_y H_z^* \right)_A \\ &= \int dk_y \int dk_z \left| \frac{F(k_y) G(k_z)}{2\pi L_z} \right|^2 \left( \frac{-E_y(k_y, k_z)}{K_0} \right)_A. \end{aligned} \quad (6)$$

The first term in the integrand depends only upon the dimensions of the current sheet and the chosen variations of the current with  $y$  and  $z$ . The second term  $[-E_y(k_y, k_z)/K_0]_A \equiv Z_k$  may be called the intrinsic spectral impedance of the antenna; it is found to be given by (in MKS units):

$$\sqrt{\frac{\epsilon_0}{\mu_0}} Z_k = \frac{(e^{2A} - 1)}{2(e^{2C} - 1)} \left[ (e^{2B} - 1) \frac{1 - n_y^2}{n_\alpha} - 2e^{2B}(e^{2A} - 1) n_\alpha \frac{\mathfrak{S}}{D} \right] \quad (7)$$

where

$$D = (e^{2C} + 1) \left[ (n_z^2 - 1) \mathfrak{S} - n_\alpha \mathfrak{H} \tanh C \right] \quad (8)$$

$$\mathfrak{H} = \frac{i}{n_{yz}^2 - K_\perp(\xi_{\text{scr}})} \left\{ n_y K_\times(\xi_{\text{scr}}) \mathfrak{S} + \left[ n_z^2 - K_\perp(\xi_{\text{scr}}) \right] \alpha_2^{1/3} \mathfrak{S}' \right\} \quad (9)$$

$$\mathfrak{S} = \text{Ai}(\tau_{\text{scr}}) - i \text{Bi}(\tau_{\text{scr}}); \tau_{\text{scr}} = -\frac{\alpha_1}{\alpha_2^{2/3}}; \mathfrak{S}' = \frac{d\mathfrak{S}}{d\tau} \Big|_{\tau=\tau_{\text{scr}}} \quad (10)$$

$n_\alpha = (1 - n_{yz}^2)^{1/2}$ , and  $A = -ik_0 n_\alpha a$ ,  $B = -ik_0 n_\alpha b$ ,  $C = A + B$ .

The spectrum of the electric field excited in the plasma, as given by (4), is found by determining  $E_0$ ; the result is

$$\sqrt{\frac{\epsilon_0}{\mu_0}} \frac{E_0}{K_0} = (e^{2A} - 1) e^{B \frac{n_\alpha}{D}} F(n_y) G(n_z) \quad (11)$$

The time-averaged power flow density spectrum into the plasma ( $x$ -direction) is given by

$$\langle s_x \rangle = \frac{1}{2} \sqrt{\frac{\epsilon_0}{\mu_0}} \left( \frac{n_z^2 - K_\perp}{n_{yz}^2 - K_\perp} \right) \text{Im} \left( E_y^* \frac{dE_y}{d\xi} \right) \quad (12)$$

and asymptotically in  $\xi$  (i.e. beyond the cutoff near the screen)  $\text{Im}(E_y^* dE_y/d\xi) \approx (\alpha_2^{1/3}/\pi) |E_0|^2$ . The total time-averaged power flowing into the plasma is then  $P_{pl} = \int (dk_y/2\pi) \int (dk_z/2\pi) \langle s_x \rangle$ .

The results will now be applied to an ICRF antenna for a large tokamak such as JET: major radius =  $3m$ , minor radius (to the screen) =  $1.27m$ , parabolic density profile with peak density =  $5 \times 10^{13} cm^{-3}$ , density at the screen,  $n_s = 2 \times 10^{11} cm^{-3}$ , toroidal magnetic field =  $35kG$ ,  $\omega = 2\Omega_{D0} = 3.35 \times 10^8 sec^{-1}$ . For  $a = 5cm$  and  $b = 3cm$ , the intrinsic spectral impedance,  $Z_k$ , is shown as a function of  $n_y$  and  $n_z$  in Figure 2. In order to maximize  $Z_A$ , Fig. 2 indicates the Fourier spectrum of the current profile has to extend uniformly over a wider range in  $n_y$  than in  $n_z$ . The major contribution to  $Z_k$  from  $n_z$  is seen to be limited to  $|n_z| \leq 5$ . Figure 3 shows  $Z_k$  as a function of  $n_z$  for various  $n_y$ . It is symmetric about  $n_z = 0$ . Choosing  $L_y = 60cm$ ,  $L_z = 40cm$  and a uniform current profile in the  $y$ - $z$  directions, we find  $Z_A \approx 21\Omega$ , and the electric field spectrum in the plasma as shown in Fig. 4. If, instead, we use  $L_y = (\lambda_0/4) = (\pi c/2\omega) \approx 140cm$  and  $L_z = 6cm$  with a uniform current profile in the  $z$ -direction and a quarter sinc-wave in the  $y$ -direction, there is no significant change in the value of  $Z_A$ . This is an indication of the narrow spread in  $n_z$  of  $Z_k$ .

The impedance,  $Z_A$ , is sensitive to the dimensions  $a$ ,  $b$  and the density at the screen. If we choose  $a = 5cm$ ,  $b = 3cm$ ,  $L_y = 60cm$ ,  $L_z = 40cm$  and a uniform current profile in  $y$ - $z$  directions but change  $n_s$  to  $5 \times 10^{11} cm^{-3}$  the impedance drops to  $12\Omega$ .  $Z_A$  increases with increasing  $a$  until it reaches a maximum value of  $48\Omega$  (for  $n_s = 2 \times 10^{11} cm^{-3}$ ). Keeping  $a = 5cm$  and increasing  $b$  to  $10cm$ ,  $Z_A$  drops to  $5\Omega$  (for  $n_s = 2 \times 10^{11} cm^{-3}$ ).

From our numerical calculations we find that ignoring  $n_y$  in the evaluation of the impedance has a significant effect. If we let  $n_y = 0$ , then for the case of the uniform current profile with  $L_z = 40cm$ ,  $a = 5cm$ ,  $b = 3cm$ , and  $n_s = 2 \times 10^{11} cm^{-3}$ , the impedance per unit antenna length in the  $y$ -direction is  $6.7\Omega/m$ . This gives an impedance for  $L_y = 60cm$  of  $4\Omega$  compared to  $21\Omega$  when we account for the appropriate spectrum in  $n_y$ .

## References

- [1] A. Bers, J. Jacquinet, and G. Lister, *Proceedings 2nd Annual Joint Grenoble-Varenna International Symposium*, Como, 3-12 September 1980. Also, Report EUR-CEA-FC 1066, Association Euratom-C.E.A., Fontenay-aux-Roses, France, September 1980.

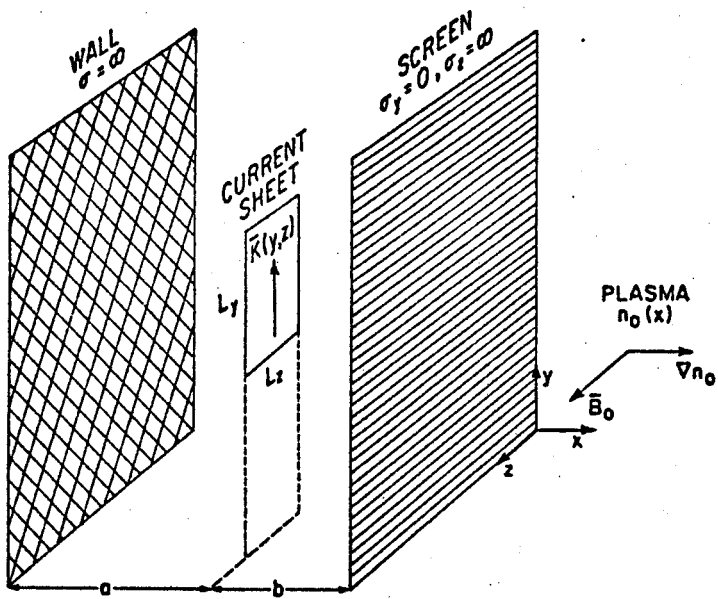


FIGURE 1

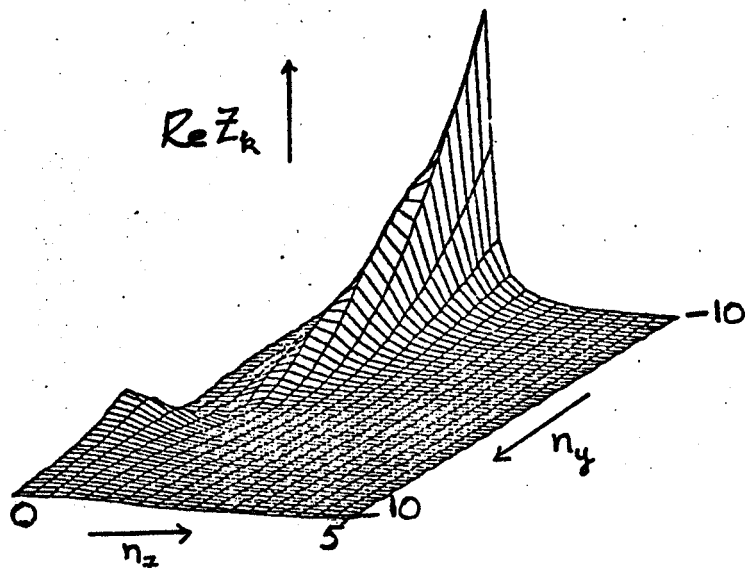


FIGURE 2

Intrinsic Spectral Impedance

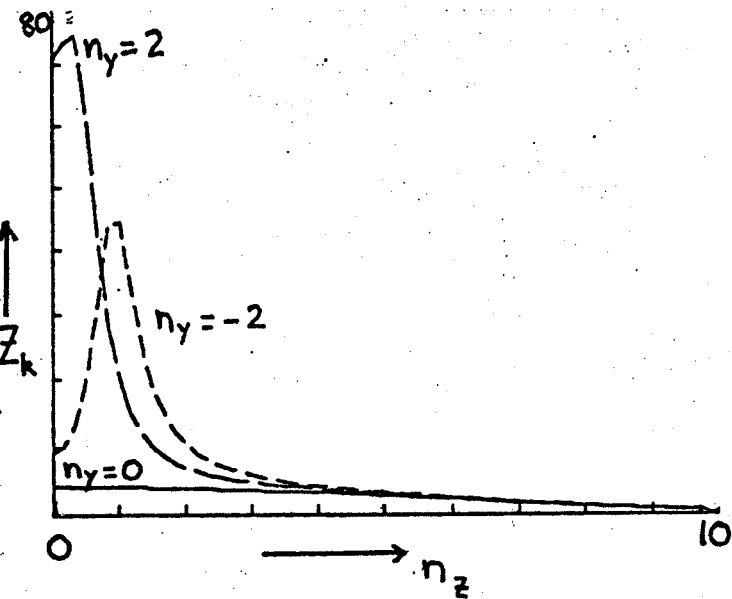


FIGURE 3

Intrinsic Spectral Impedance

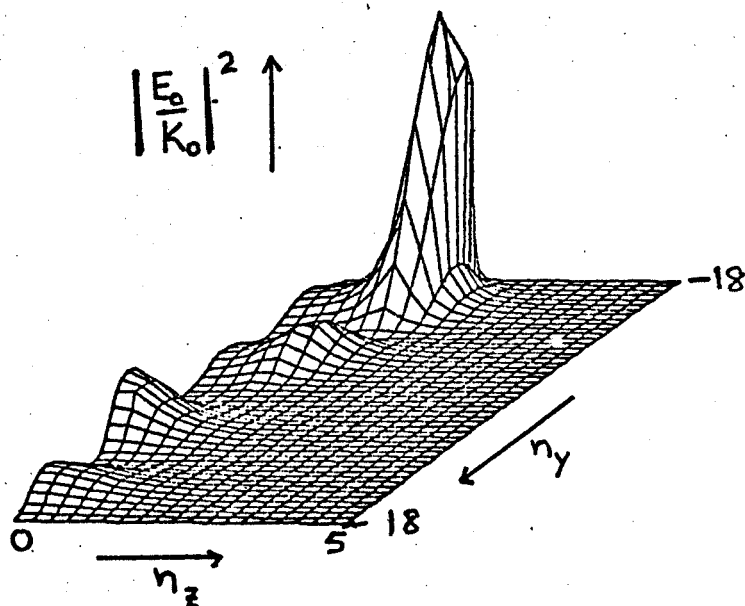


FIGURE 4

Amplitude of the electric field inside the plasma.